**Clinical Orthopaedics
and Related Research®**
A Publication of The Association of Bone and Joint Surgeons®

BASIC RESEARCH

Bone Microarchitecture of the Talus Changes With Aging

Matthias Krause MD, Martin Rupprecht MD,
Marcus Mumme MD, Klaus Püschel MD,
Michael Amling MD, Florian Barvencik MD

Abstract

Background   Fractures of the talus in the elderly are rare and usually result from high-impact injuries, suggesting only minor age-related bone structure changes. However, total ankle replacement failures with age often result from talar subsidence, suggesting age-related bone loss in the talus. Despite a number of histological analyses of talar microarchitecture, the effects of age and sex on talar microarchitecture changes remain poorly defined.

Questions/purposes   The aim of this study was to analyze changes or differences in the trabecular microarchitecture of the talus with regard to (1) age and (2) sex.

Methods   Sixty human tali were harvested from 30 patients at autopsy of three different age groups (20–40, 41–60, 61–80 years). The specimens were analyzed by radiography, micro-CT, and histological analysis. Given that there was no difference between the left and right talus, static histomorphometric parameters were assessed in three regions of interest of the right talus only (body, neck, head; n = 30).

Results   The talar body, neck, and head were affected differently by age-related changes. The greatest loss of bone volume with age was seen in the talar body (estimate: -0.239; 95% confidence interval [CI], -0.365 to -0.114; $p < 0.001$). In the talar neck (estimate: -0.165; 95% CI, -0.307 to -0.023; $p = 0.025$), bone loss was only moderate and primarily was the result of reduction in trabecular thickness (estimate: -1.288; 95% CI, -2.449 to -0.127; $p = 0.031$) instead of number (estimate: -0.001; 95% CI, -0.005 to -0.003; $p = 0.593$). Bone structure changes were independent of sex.

Conclusions   Age-related bone structure changes predominantly occur in the talar body, which poses a potential risk factor for total ankle replacement loosening. The moderate changes in the talar neck might explain the persistent low incidence of talar neck fractures with age.

M. Krause, M. Mumme, M. Amling (✉), F. Barvencik
Department of Osteology and Biomechanics, University Medical Center Hamburg-Eppendorf, Lottestr. 52, 22529 Hamburg, Germany
e-mail: amling@uke.de

M. Rupprecht
Department of Pediatric Orthopaedic Surgery, Children's Hospital Hamburg-Altona, Hamburg, Germany

K. Püschel
Department of Legal Medicine, University Medical Center Hamburg-Eppendorf, Hamburg, Germany

Clinical Relevance   Our findings suggest that before total ankle replacement implantation, careful patient selection with dual-energy xray absorptiometry evaluation may be necessary to reduce the risk of talar implant subsidence.

Introduction

The talus has a unique internal architecture as a result of its distinguished function as a "bony meniscus" bearing and transmitting the total weight of the body through the bone. The talus has no attachments of muscles, or fasciae, which could support the absorption of applied loads [2, 27]. Hence, its microarchitecture reflects its sole ability to endure great compressive and tensile forces during walking, running, and jumping distributing them from the talus to the adjacent bones and therefore varies in different regions of interest (ROIs) [4, 34, 39]. Because the talar body has a pronounced subchondral bone lamella, enormous axial loading forces resulting from high-impact injuries are necessary to cause talar fractures [21, 27, 36]. Talar body fractures account for only 10% to 20% of all talus fractures [6, 15, 27]. In contrast, the talar neck is a place of decreased resistance to injury compared with the talar body or head as a result of a weaker cortical shell. This may explain its involvement in almost 50% of all talar fractures [29, 33]. Overall, although fractures of the talus account for fewer than 1% of all bony fractures [27] and 3% to 6% of all foot fractures [1], they constitute serious injuries [3]. After a talar fracture, avascular necrosis is a major complication potentially leading to posttraumatic arthritis and chronic pain in turn potentially leading to ankle fusion or total ankle replacement [3, 20].

Sufficient bone stock is a prerequisite for durability of total ankle replacements [14]; supporting this idea is the fact that one of the most common reasons for implant failure is talar subsidence resulting from periprosthetic osteolysis from polyethylene wear or direct mechanical insufficiency of the underlying bone stock [19, 40]. Therefore, given that the mean patient age at total ankle replacement implantation is between 50 and 60 years, knowledge of a potential age effect on bone quality of the talus is of paramount importance [23, 42]. It is noteworthy that the anatomical partner of the talus for conferring the contact energy of the foot to the ground, the calcaneus, displays age-related changes in its microarchitecture similar to the proximal humerus or the distal radius [7, 8, 37]. Although there have been a number of histological analyses of talar microarchitecture, the effects of age and sex on talar microarchitecture changes remain poorly characterized [4, 18, 21, 34, 39].

We therefore sought to analyze changes or differences in the trabecular microarchitecture of the talus with regard to (1) age and (2) sex.

Materials and Methods

Autopsy Specimens and Sample Preparation

Sixty tali were harvested from 30 age- and sex-matched patients at autopsy within 48 hours after death (five women and five men each per age groups 20–40 years [younger], 41–60 years [mid-age], 61–80 years [older]) ruling out any major decay of bone structure quality. All bone donors died in accidents or of acute disease. Iliac crest biopsies were obtained from all autopsy cases to exclude any metabolic diseases known to affect the skeleton. Review of hospital records and whole-body autopsy reports were used to exclude individuals with bone cancer, diabetes, glucocorticoid medication, severe kidney disease, periods of longer immobilization, or donors on other drugs known to affect calcium metabolism. No specimens with osteoarthritis were included in the study group. A 4-mm central slice of the talus was sectioned in the sagittal plane using a diamond-coated band saw (Exakt, Norderstedt, Germany). Before further preparation, one section of each age group was exemplarily scanned by micro-CT (μCT40; SCANCO Medical AG, Bruettisellen, Switzerland) with an in vitro scanning protocol (55 kVp, 145 μA, 200-ms integration time) resulting in an isotropic voxel size of 18 μm to visualize three-dimensional bone histomorphometry. After documentation on contact radiographs, the specimens were subjected to an undecalcified infiltration process, ground to a thickness of 1 mm, and stained using a modification of the von Kossa method [13, 31]. ROIs were defined by two lines: (1) running from the distal border from the inflow of the arteria sinus tarsi to the caudal end of the facies articularis navicularis; and (2) running from the distal end of the trochlea tali (facies articularis superior) to the distal end of the facies articularis calcanea posterior. These two lines divide the specimens into three ROIs (body, neck, and head; Fig. 1). Depending on the macroscopic size of the individual talar ROI analyzed, the ROIs were located in the same position and therefore individually varied in size. Informed consent was obtained from the family members after comprehensive information on all connected issues. This study was approved by the Ethics Committee of the Hamburg Chamber of Physicians and was carried out according to existing rules and regulations of the University Medical Center Hamburg-Eppendorf (PV3486).

Histomorphometry

Two- and three-dimensional analysis was carried out by dark and light field microscopy using a stereo microscope (Zeiss GmbH, Göttingen, Germany) on the ground specimens according to ASBMR standards [17]. Cortical bone
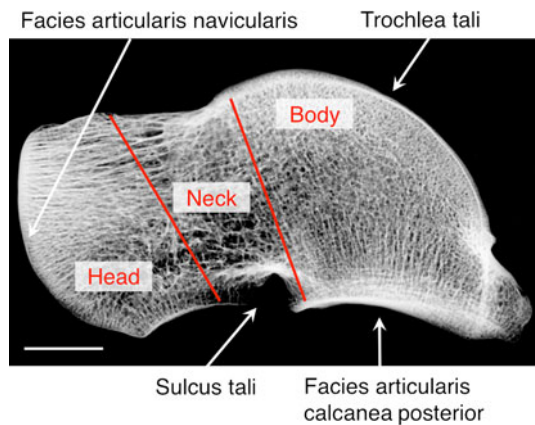
Fig. 1 A contact radiograph of the talus depicts the three regions of interest in the sagittal plane (bar = 1 cm).

as well as the subcortical region (1 mm trabecular bone) was omitted from the histomorphometric analysis. The following parameters were analyzed: bone volume fraction (%), trabecular number (mm^{-1}), trabecular thickness (µm), and trabecular separation (mm).

Statistical Methods

Statistical analysis was carried out using IBM® SPSS® Statistics 19 (SPSS Inc, Chicago, IL, USA). Preliminary analysis revealed no statistically significant difference between the right and left talus in any of the outcome variables. Hence, we report the results of the right talus only (n = 30). Mean values ± SDs are reported for all parameters. Multivariate analyses of covariance were conducted to determine the influence of age and sex each as a metric variable on the microarchitecture of the talus. Subsequent separate linear regression with the presentation of estimates of their corresponding 95% confidence intervals was used to determine the association between metric variables. To study the extent of microarchitectural changes at different ages, age was also defined as a categorical variable with regard to younger, mid, and older age. Student's t-test was used to report mean differences and percentage changes. Univariate analysis of variance and Tukey's honestly significant difference post hoc assessment were used for comparison of different ROIs within the same age group. All tests were two-sided and a p value of < 0.05 was considered significant.

Results

Histomorphometry

Histological analysis revealed an age-related bone loss, which affected the body, neck, and head differently

(Fig. 2). There was no association between bone structure changes and sex (Table 1).

Bone Volume Fraction

Bone volume was highest in the talar head and lowest in the talar body, which reached statistical significance in the older age group (p = 0.027; Table 2). Hence, the age-related percentage bone volume decrease was highest in the talar body (estimate: −0.239; 95% confidence interval [CI], −0.365 to −0.114; r^2 = 0.35; p < 0.001) and moderate in the neck (estimate: −0.165; 95% CI, −0.307 to −0.023; r^2 = 0.17; p < 0.05) and head (estimate: −0.170; 95% CI, −0.326 to −0.014; r^2 = 0.15; p < 0.05; Table 3; Fig. 3). Comparing the younger and mid-age groups, bone loss was similar for all ROIs (body 16%, neck 9%, head 16%). In contrast, the additional bone loss between the mid- and older age groups varied in the different ROIs but the differences did not attain statistical significance (body −19%, neck −8%, head −3%; Fig. 4).

Trabecular Number

The talar neck demonstrated the significantly lowest number of trabeculae in the younger and mid-age groups (each p < 0.05; Table 2). There was no age-related loss of trabecular number in the talar neck or head (r^2 = 0.01) but in the talar body (estimate: −0.006; 95% CI, −0.011 to −0.001; r^2 = 0.15; Table 3; Fig. 3), which was higher in the older than in the mid-age group (Fig. 4). This again did not attain statistical significance.

Trabecular Thickness

In the younger age group, plates were the predominant structural element in the neck and head, whereas in the body, rod-like structures characterized the trabecular microarchitecture. There was a transition of small inter-anastomizing plates coming from the talar body to regularly arranged thicker plates to the talar head. An age-related thickness loss in all ROIs, which was greatest in the talar body (r^2 = 0.37, neck r^2 = 0.16, head r^2 = 0.19, all p < 0.05; Table 3; Fig. 3), was detected. In the head and neck, the trabecular thickness decrease was similar among different age groups (Fig. 4). In contrast, in the body, the trabecular thickness decrease was significantly higher between the younger and mid-age groups (−14.3%, p = 0.045) but only moderate higher between the mid- and older age groups (−8.3%, p = 0.156; Fig. 4).
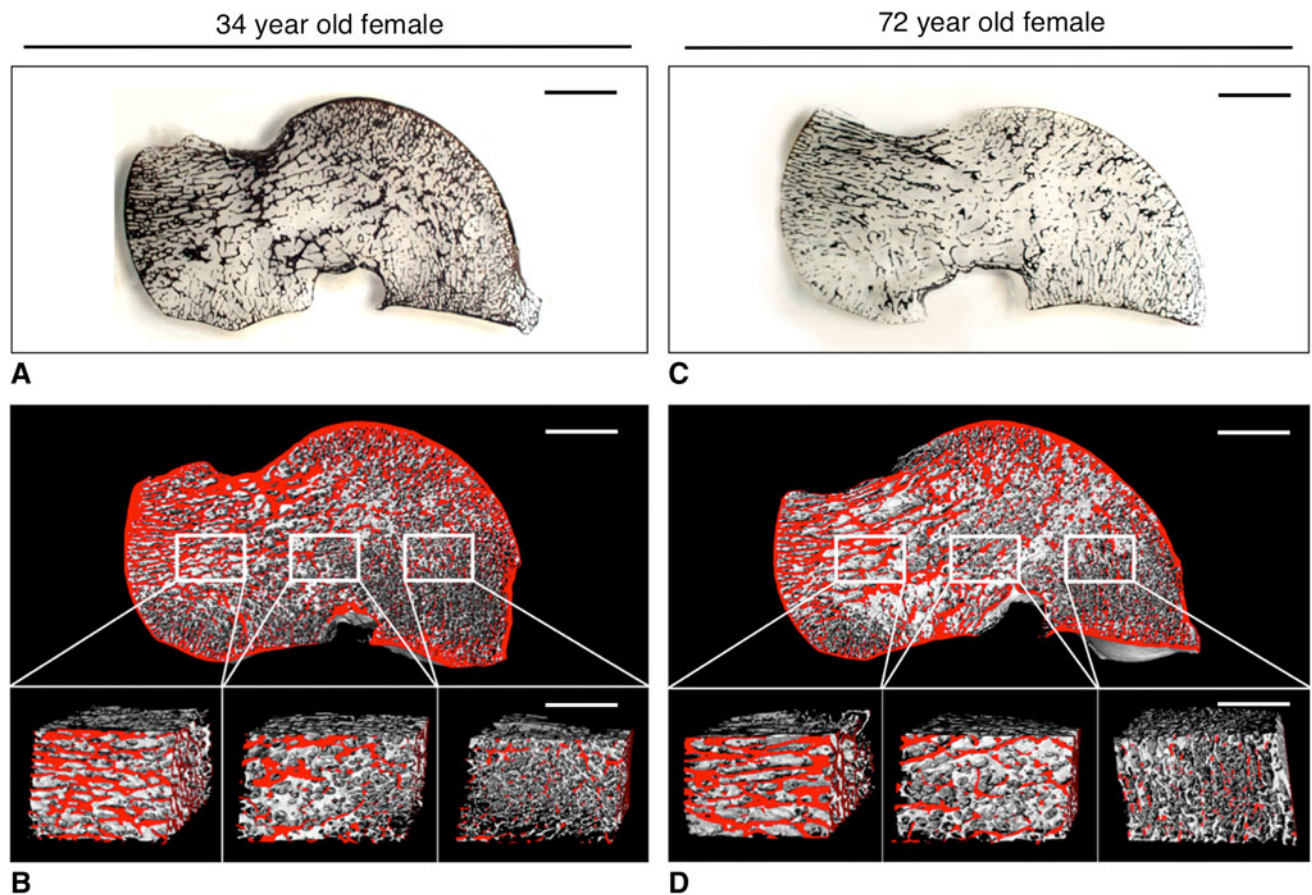
34 year old female

72 year old female

Fig. 2A–D Two-dimensional and three-dimensional illustrations of the age-related bone visualize the structural deterioration of the talus. The left panel indicates the two sets of plate-like trabeculae running from the trochlea tali to the (1) calcaneal facet and (2) to the neck and head of the talus in a 34-year-old woman (**A**, 1 mm thick, undecalcified, von Kossa-stained block grinding; bar = 1 cm). Three-dimensional visualization reveals the various structural characteristics of the respective ROIs: the body, the neck, and the talar head (**B**, μCT40 image, bone at the surface if colored red; bar = 1 cm). In contrast, the right panel demonstrates the predominant bone loss in the talar body of a 72-year-old woman (**C**, 1 mm thick, undecalcified, von Kossa stained block grinding; bar = 1 cm). However, despite age-related bone loss, three-dimensional visualization reveals the intact structural integrity of the talar neck and head (**D**, μCT40 image, bone at the surface if colored red; bar = 1 cm). The structural characteristics of the individual regions of interest are highlighted in the magnifications again (bar = 5 mm).

Table 1. Association among histomorphomtric parameters, age (metric), and sex after analysis of covariance and its corresponding p values

ROI	Independent variable	BV/TV (%)	Tb.N (mm^{-1})	Tb.Th (μm)	Tb.Sp (mm)
Body	Age	0.001	0.036	0.001	0.017
	Sex	NS	NS	NS	NS
Neck	Age	0.028	NS	0.031	NS
	Sex	NS	NS	NS	NS
Head	Age	0.027	NS	0.008	NS
	Sex	NS	NS	NS	NS

ROI = region of interest; BV/TV = bone volume fraction; Tb.N = trabecular number; Tb.Th = trabecular thickness; Tb.Sp = trabecular separation; NS = nonsignificant.

Trabecular Separation

Trabecular separation was significantly higher in the talar neck when compared with the head and body in the younger and mid-age groups ($p < 0.05$; Table 2). There was no age-related increase of trabecular separation in the neck or head (neck $r^2 = 0.07$, head $r^2 = 0.05$) primarily as a result of a constant trabecular number. Trabecular separation increased

Table 2. Histomorphometric analysis of the talus (mean ± SD)

ROI	Age group	BV/TV (%)	Tb.N (mm^{-1})	Tb.Th (μm)	Tb.Sp (mm)
Body	Younger	26.25 ± 5.39	1.41 ± 0.17[†]	185.18 ± 25.95[†,‡]	0.532 ± 0.099[†]
	Mid-age	22.07 ± 4.74	1.39 ± 0.14[†]	158.88 ± 28.68[†,‡]	0.569 ± 0.094[†]
	Older	18.02 ± 6.40[‡]	1.24 ± 0.34	142.16 ± 21.26[†,‡]	0.741 ± 0.351
Neck	Younger	28.11 ± 6.07	1.04 ± 0.11[*,‡]	263.21± 38.90[*,‡]	0.685 ± 0.114[*,‡]
	Mid-age	25.56 ± 6.69	1.00 ± 0.14[*,‡]	252.46 ± 48.82[*]	0.760 ± 0.165[*,‡]
	Older	23.49 ± 6.08	1.08 ± 0.19[‡]	219.80 ± 59.73[*]	0.736 ± 0.176
Head	Younger	31.01 ± 6.02	1.38 ± 0.20[†]	225.30 ± 35.21[*,†]	0.515 ± 0.115[†]
	Mid-age	26.73 ± 7.29	1.27 ± 0.15[†]	209.41 ± 48.26[*]	0.590 ± 0.123[†]
	Older	25.89 ± 6.64[*]	1.37 ± 0.20[†]	187.49 ± 31.00[*]	0.558 ± 0.130

* Interage group p < 0.05 compared with body after analysis of variance (ANOVA) and Tukey's honestly significant difference (HSD) post hoc test; [†]interage group p < 0.05 compared with neck after ANOVA and Tukey's HSD post hoc test; [‡]interage group p < 0.05 compared with head after ANOVA and Tukey's HSD post hoc test; ROI = region of interest; BV/TV = bone volume fraction; Tb.N = trabecular number; Tb.Th = trabecular thickness; Tb.Sp = trabecular separation.

Table 3. Linear regression analysis between histomorphometric parameters of the talus and age (years)

ROI	Parameter	Intercept	Estimate (95% confidence interval)	p value
Body	BV/TV (%)	36.343	−0.239 (−0.365 to −0.114)	< 0.001
	Tb.N (mm^{-1})	1.640	−0.006 (−0.011 to −0.001)	0.033
	Tb.Th (μm)	220.043	−1.167 (−1.763 to −0.571)	< 0.001
	Tb.Sp (mm)	0.293	0.006 (0.001–0.012)	0.014
Neck	BV/TV (%)	33.913	−0.165 (−0.307 to −0.023)	0.025
	Tb.N (mm^{-1})	1.096	−0.001 (−0.005 to 0.003)	NS
	Tb.Th (μm)	309.297	−1.288 (−2.449 to −0.127)	0.031
	Tb.Sp (mm)	0.597	0.003 (−0.001 to 0.006)	NS
Head	BV/TV (%)	36.343	−0.170 (−0.326 to −0.014)	0.034
	Tb.N (mm^{-1})	1.400	−0.001 (−0.006 to 0.003)	NS
	Tb.Th (μm)	263.727	−1.131 (−2.024 to −0.238)	0.015
	Tb.Sp (mm)	0.467	0.002 (−0.001 to 0.005)	NS

ROI = region of interest; BV/TV = bone volume fraction; Tb.N = trabecular number; Tb.Th = trabecular thickness; Tb.Sp = trabecular separation; NS = not significant.

significantly in the talar body with advancing age (estimate: 0.006; 95% CI, 0.001–0.012; r^2 = 0.20; p = 0.014; Table 3; Fig. 3).

Discussion

Given its importance in the ankle and the severe consequences when injuries occur, it is important to understand the unique architecture of the talus. The subsidence of the talar component in total ankle arthroplasty is an important reason for implant failures in older patients, which leaves open the question as to whether some age-related changes do occur. Despite previous descriptions of the talar microarchitecture, these studies were either just descriptive in nature [4, 21, 34] or focused on the evaluation of the talar body only [18, 26, 39] without consideration of age- or

sex-related differences. In this study, we were able to show an age-related talar bone loss, which predominantly affects the talar body rather than the neck or head, regardless of sex.

This study has some limitations. First, we quantified trabecular structure in the sagittal plane only; previous reports described the talar microarchitecture in sagittal, coronal, and horizontal planes [4, 39]. As a result of specimen destruction during histological preparation, there was no additional bone stock available for the analysis of other planes. However, the transition of trabeculae from the talar body to the head and neck or to the calcaneal facet transferring the load was demonstrated following tensile and compression forces [4, 10]. Therefore, the evaluation of only one plane was needed to study age- and sex-related changes of the talar body, neck, and head simultaneously. The potential gain of information by the analysis of additional planes is limited and was previously performed for
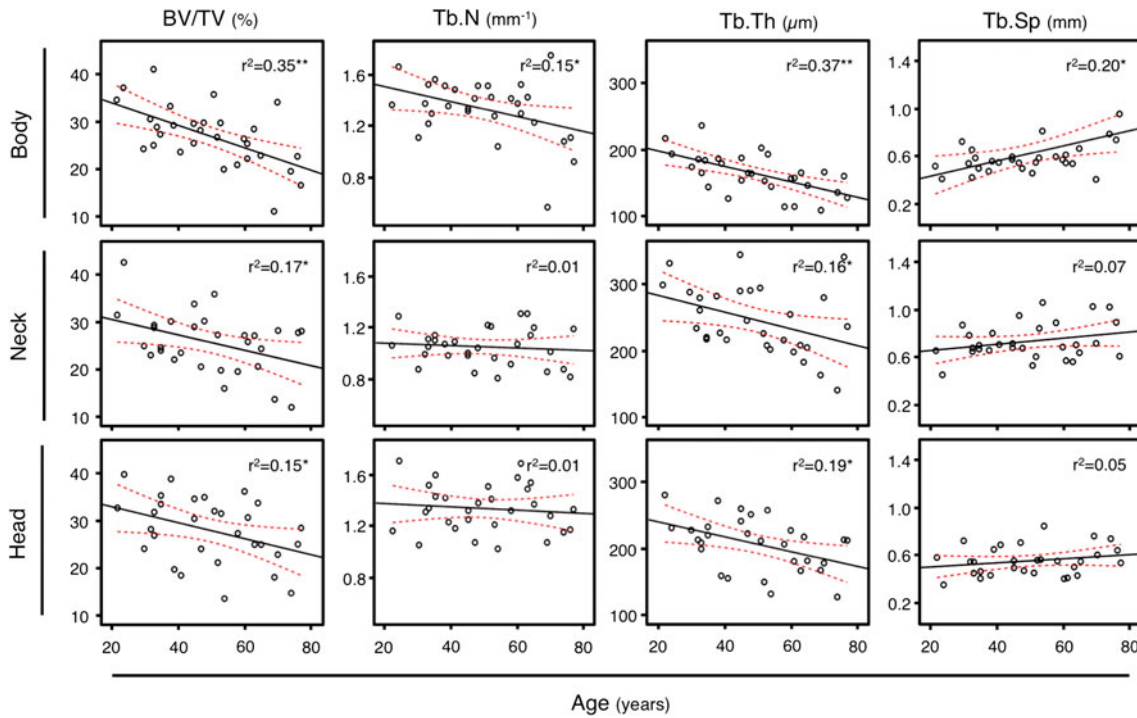
Fig. 3 The slopes of the depicted regression analyses of the histomorphometric parameters and age for the respective ROIs (talar body, neck, and head) are represented by the black solid lines. In red the 95% confidence intervals are illustrated. BV/TV = bone volume fraction; Tb.N = trabecular number; Tb.Th = trabecular thickness; Tb.Sp = trabecular separation.

Fig. 4 Percentage changes of the histomorphometric outcome variables are illustrated according to specific regions of interest comparing bone loss between younger and mid-age as well as mid-age and older bone donors. BV/TV = bone volume fraction; Tb.N = trabecular number; Tb.Th = trabecular thickness; Tb.Sp = trabecular separation.
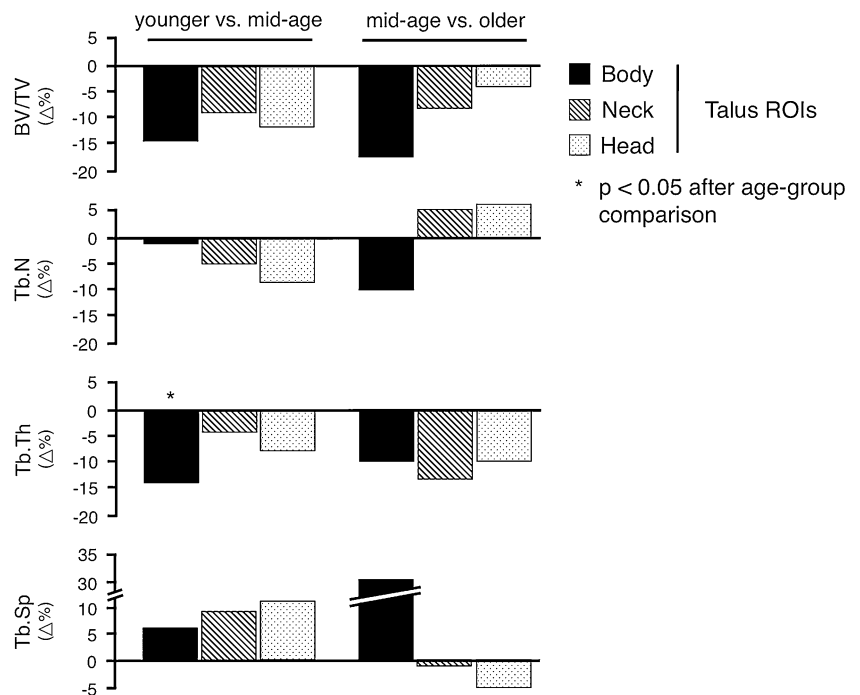
descriptive reasons only [4]. Given that the analysis of additional planes would also increase the number of cases needed, which might ethically be hard to justify, we chose to study the sagittal plane only. Second, despite the review of all medical records to exclude bone-affecting diseases and medication, there was no assessment of areal bone mineral density to diagnose osteoporosis according to World Health Organization standards. However, after evaluating iliac crest biopsies, no severe bone structure deterioration was observed in any of the bone donors in this

series. This was supported by the fact that even in the older age group, no significant differences between males and females were observed appreciating that osteoporosis primarily affects postmenopausal women [32]. Third, there were no cases with osteoarthritis (OA) in the study group although the most common indications for implantation of total ankle arthroplasty are posttraumatic arthritis and primary OA [30]. The impact of OA on subchondral bone is well established, especially in the femoral head and the proximal tibia. An increased bone volume fraction, trabecular number, trabecular separation as well as bone mineralization were described and therefore a stabilizing effect for implant duration is conceivable [11, 16, 28]. Jordan et al. [28] have also found an increased trabecular area at the intertrochanteric femoral neck in patients with OA compared with healthy control subjects. With respect to standard ASBMR histomorphometric parameters, other reports were not able to demonstrate intertrochanteric differences between patients with OA and control subjects [17, 22, 44]. Therefore, in contrast to the recognized impact of OA on subchondral bone, the effect of OA on bone regions deeper to the affected articular bone region is not well established. Modern surgical techniques attempt to preserve as much bone as possible at implantation. Nonetheless, to create a large bone-implant interface, parts of the subchondral bone plate are resected and bone regions deeper to the subchondral bone plate are responsible for implant stabilization. Hence, next to the accepted influence of implant design and surgical technique on implant survival, mechanically sufficient bone stock is needed for long-term total ankle arthroplasty survival [30]. Accordingly, the age-related changes of bone deeper to the subchondral lamella might influence the long-term stability of the total ankle arthroplasty.

Our observations suggested an age-related talar bone loss. This is consistent with results of other skeletal sites such as the distal radius, proximal humerus, and the calcaneus [7, 8, 37]. Interestingly, the extent of structural changes differed among the three ROIs. The greatest bone loss was seen in the body resulting from a transition of mainly plate-like to more rod-like trabeculae. Instead, in the neck and head, the trabeculae remained plate-like with increasing age. Here, the transfer of vertical loading forces into tensile forces while standing and walking might have prevented major age-related bone deteriorations. Hence, the ROI-specific bone loss might be the result of different mechanical loading conditions [5, 7, 35]. Because the distribution of compressive and tensile forces through the talus does not severely change with age, we speculate that the differently sized volumes of interest might be responsible for the greater bone loss in the body [34]. At first glance, the nearly unimpaired bone structure of the talar neck seemed contradictory given that the femoral neck has

a similar weight-transmitting function and an age-related degradation of the femoral neck was reported [10, 12]. Age-related cortical trabecularization and thinning were attributed to a higher risk of hip fracture in the elderly [9, 10]. However, talar neck fractures have a low incidence at older age and are primarily seen in patients with a high-impact trauma [25, 36]. In contrast to the femoral neck, the cortical bone of the talar neck is rather small [4, 34]. Therefore, plate-like trabeculae rather than the cortical shell most probably contribute to bone strength. Given that the number of trabeculae was not changed with age and thickness decreased only moderately, the overall structural integrity of the talar neck was principally preserved with age. Next to a reduced exposure to high-impact sports or accidents, the basically preserved bony architecture might explain the persistent low incidence of talar neck fractures in older people. By contrast, total ankle replacement, which has become more popular as a comparable degree of pain reduction and even better function than common ankle arthrodesis was shown [24, 38], may be affected by the changes we observed to the talar body. The most common complication after ankle replacement is aseptic loosening, with 55% with subsidence of the talar component into the talar body being one of the main reasons for failure [19, 41, 43]. The age-related changes we observed may help to explain this finding.

This study failed to find a sex-specific difference, which is in accordance with histomorphometric results of the calcaneus as one partner of load transmission of the talus where also no differences between males and females were observed [37]. In contrast, sex-specific bone structure differences have been primarily found in less mechanically loaded skeletal sites such as the humeral head or the distal radius [7, 8].

Our study demonstrated that the talus is subjected to age-related bone structure changes, which primarily affect the talar body rather than the neck or head, and are independent of sex. The modest structural deterioration of the talar neck may explain the unchanged incidence of talar neck fractures with age. By contrast, the distinctive loss of bone volume in the talar body may constitute a relevant risk factor for increased failure of the talar component in total ankle replacement and suggest careful patient selection with dual xray absorptiometry evaluation to ensure long-term success for implant survival.

References

1. Adelaar RS. The treatment of complex fractures of the talus. *Orthop Clin North Am.* 1989;20:691–707.
2. Adelaar RS. Fractures of the talus. *Instr Course Lect.* 1990;39:147–156.

3. Ahmad J, Raikin SM. Current concepts review: talar fractures. *Foot Ankle Int.* 2006;27:475–482.

4. Athavale SA, Joshi SD, Joshi SS. Internal architecture of the talus. *Foot Ankle Int.* 2008;29:82–86.

5. Barak MM, Lieberman DE, Hublin JJ. A Wolff in sheep's clothing: trabecular bone adaptation in response to changes in joint loading orientation. *Bone.* 2011;49:1141–1151.

6. Barnett TM, Teasdall RD. Bilateral lateral process fracture of the talus in a motocross rider. *Foot Ankle Int.* 2008;29:245–247.

7. Barvencik F, Gebauer M, Beil FT, Vettorazzi E, Mumme M, Rupprecht M, Pogoda P, Wegscheider K, Rueger JM, Pueschel K, Amling M. Age- and sex-related changes of humeral head microarchitecture: histomorphometric analysis of 60 human specimens. *J Orthop Res.* 2010;28:18–26.

8. Beil FT, Barvencik F, Gebauer M, Mumme M, Beil B, Pogoda P, Rueger JM, Puschel K, Amling M. The distal radius, the most frequent fracture localization in humans: a histomorphometric analysis of the microarchitecture of 60 human distal radii and its changes in aging. *J Trauma.* 2011;70:154–158.

9. Bell KL, Loveridge N, Power J, Garrahan N, Stanton M, Lunt M, Meggitt BF, Reeve J. Structure of the femoral neck in hip fracture: cortical bone loss in the inferoanterior to superoposterior axis. *J Bone Miner Res.* 1999;14:111–119.

10. Blain H, Chavassieux P, Portero-Muzy N, Bonnel F, Canovas F, Chammas M, Maury P, Delmas PD. Cortical and trabecular bone distribution in the femoral neck in osteoporosis and osteoarthritis. *Bone.* 2008;43:862–868.

11. Bobinac D, Spanjol J, Zoricic S, Maric I. Changes in articular cartilage and subchondral bone histomorphometry in osteoarthritic knee joints in humans. *Bone.* 2003;32:284–290.

12. Boutroy S, Vilayphiou N, Roux JP, Delmas PD, Blain H, Chapurlat RD, Chavassieux P. Comparison of 2D and 3D bone microarchitecture evaluation at the femoral neck, among postmenopausal women with hip fracture or hip osteoarthritis. *Bone.* 2011;49:1055–1061.

13. Breer S, Krause M, Busse B, Hahn M, Ruther W, Morlock MM, Amling M, Zustin J. Analysis of retrieved hip resurfacing arthroplasties reveals the interrelationship between interface hyperosteoidosis and demineralization of viable bone trabeculae. *J Orthop Res.* 2012;30:1155–1161.

14. Calderale PM, Garro A, Barbiero R, Fasolio G, Pipino F. Biomechanical design of the total ankle prosthesis. *Eng Med.* 1983;12:69–80.

15. Cantrell MW, Tarquinio TA. Fracture of the lateral process of the talus. *Orthopedics.* 2000;23:55–58.

16. Christensen P, Kjaer J, Melsen F, Nielsen HE, Sneppen O, Vang PS. The subchondral bone of the proximal tibial epiphysis in osteoarthritis of the knee. *Acta Orthop Scand.* 1982;53:889–895.

17. Dempster DW, Compston JE, Drezner MK, Glorieux FH, Kanis JA, Malluche H, Meunier PJ, Ott SM, Recker RR, Parfitt AM. Standardized nomenclature, symbols, and units for bone histomorphometry: a 2012 update of the report of the ASBMR Histomorphometry Nomenclature Committee. *J Bone Miner Res.* 2013;28:2–17.

18. DeSilva JM, Devlin MJ. A comparative study of the trabecular bony architecture of the talus in humans, non-human primates, and Australopithecus. *J Hum Evol.* 2012;63:536–551.

19. Dunbar MJ, Fong JW, Wilson DA, Hennigar AW, Francis PA, Glazebrook MA. Longitudinal migration and inducible displacement of the Mobility Total Ankle System. *Acta Orthop.* 2012;83:394–400.

20. Ebraheim NA, Patil V, Owens C, Kandimalla Y. Clinical outcome of fractures of the talar body. *Int Orthop.* 2008;32:773–777.

21. Ebraheim NA, Sabry FF, Nadim Y. Internal architecture of the talus: implication for talar fracture. *Foot Ankle Int.* 1999;20:794–796.

22. Fazzalari NL, Kuliwaba JS, Atkins GJ, Forwood MR, Findlay DM. The ratio of messenger RNA levels of receptor activator of nuclear factor kappaB ligand to osteoprotegerin correlates with bone remodeling indices in normal human cancellous bone but not in osteoarthritis. *J Bone Miner Res.* 2001;16:1015–1027.

23. Gougoulias N, Khanna A, Maffulli N. How successful are current ankle replacements?: a systematic review of the literature. *Clin Orthop Relat Res.* 2010;468:199–208.

24. Haddad SL, Coetzee JC, Estok R, Fahrbach K, Banel D, Nalysnyk L. Intermediate and long-term outcomes of total ankle arthroplasty and ankle arthrodesis. A systematic review of the literature. *J Bone Joint Surg Am.* 2007;89:1899–1905.

25. Halvorson JJ, Winter SB, Teasdall RD, Scott AT. Talar neck fractures: a systematic review of the literature. *J Foot Ankle Surg.* 2013;52:56–61.

26. Hebert D, Lebrun R, Marivaux L. Comparative three-dimensional structure of the trabecular bone in the talus of primates and its relationship to ankle joint loads generated during locomotion. *Anat Rec (Hoboken).* 2012;295:2069–2088.

27. Higgins TF, Baumgaertner MR. Diagnosis and treatment of fractures of the talus: a comprehensive review of the literature. *Foot Ankle Int.* 1999;20:595–605.

28. Jordan GR, Loveridge N, Bell KL, Power J, Dickson GR, Vedi S, Rushton N, Clarke MT, Reeve J. Increased femoral neck cancellous bone and connectivity in coxarthrosis (hip osteoarthritis). *Bone.* 2003;32:86–95.

29. Juliano PJ, Dabbah M, Harris TG. Talar neck fractures. *Foot Ankle Clin.* 2004;9:723–736, vi.

30. Kakkar R, Siddique MS. Stresses in the ankle joint and total ankle replacement design. *Foot Ankle Surg.* 2011;17:58–63.

31. Krause M, Breer S, Hahn M, Ruther W, Morlock MM, Amling M, Zustin J. Cementation and interface analysis of early failure cases after hip-resurfacing arthroplasty. *Int Orthop.* 2012;36:1333–1340.

32. Krause M, Breer S, Mohrmann B, Vettorazzi E, Marshall RP, Amling M, Barvencik F. Influence of non-traumatic thoracic and lumbar vertebral fractures on sagittal spine alignment assessed by radiation-free spinometry. *Osteoporos Int.* 2013;24:1859–1868.

33. Lorentzen JE, Christensen SB, Krogsoe O, Sneppen O. Fractures of the neck of the talus. *Acta Orthop Scand.* 1977;48:115–120.

34. Pal GP, Routal RV. Architecture of the cancellous bone of the human talus. *Anat Rec.* 1998;252:185–193.

35. Pontzer H, Lieberman DE, Momin E, Devlin MJ, Polk JD, Hallgrimsson B, Cooper DM. Trabecular bone in the bird knee responds with high sensitivity to changes in load orientation. *J Exp Biol.* 2006;209:57–65.

36. Rammelt S, Zwipp H. Talar neck and body fractures. *Injury.* 2009;40:120–135.

37. Rupprecht M, Pogoda P, Mumme M, Rueger JM, Puschel K, Amling M. Bone microarchitecture of the calcaneus and its changes in aging: a histomorphometric analysis of 60 human specimens. *J Orthop Res.* 2006;24:664–674.

38. Saltzman CL, Mann RA, Ahrens JE, Amendola A, Anderson RB, Berlet GC, Brodsky JW, Chou LB, Clanton TO, Deland JT, Deorio JK, Horton GA, Lee TH, Mann JA, Nunley JA, Thordarson DB, Walling AK, Wapner KL, Coughlin MJ. Prospective controlled trial of STAR total ankle replacement versus ankle fusion: initial results. *Foot Ankle Int.* 2009;30:579–596.

39. Schiff A, Li J, Inoue N, Masuda K, Lidtke R, Muehleman C. Trabecular angle of the human talus is associated with the level of cartilage degeneration. *J Musculoskelet Neuronal Interact.* 2007;7:224–230.

40. Schuberth JM, Christensen JC, Rialson JA. Metal-reinforced cement augmentation for complex talar subsidence in failed total ankle arthroplasty. *J Foot Ankle Surg.* 2011;50:766–772.

41. Shi K, Hayashida K, Hashimoto J, Sugamoto K, Kawai H, Yoshikawa H. Hydroxyapatite augmentation for bone atrophy in total ankle replacement in rheumatoid arthritis. *J Foot and Ankle Surg.* 2006;45:316–321.

42. Stengel D, Bauwens K, Ekkernkamp A, Cramer J. Efficacy of total ankle replacement with meniscal-bearing devices: a systematic review and meta-analysis. *Arch Orthop Trauma Surg.* 2005;125:109–119.

43. Zhao H, Yang Y, Yu G, Zhou J. A systematic review of outcome and failure rate of uncemented Scandinavian total ankle replacement. *Int Orthop.* 2011;35:1751–1758.

44. Zupan J, Van't Hof RJ, Vindisar F, Haring G, Trebse R, Komadina R, Marc J. Osteoarthritic versus osteoporotic bone and intra-skeletal variations in normal bone: Evaluation with microCT and bone histomorphometry. *J Orthop Res.* 2013;31:1059–1066.